Acta Crystallographica Section D
Biological Crystallography
ISSN 0907-4449

Structure of cytochrome c_6 from the red alga *Porphyra yezoensis* at 1.57 Å resolution

Seiji Yamada,[a] Sam-Yong Park,[b] Hideaki Shimizu,[c] Yasutaka Koshizuka,[a] Kazunari Kadokura,[a] Tadashi Satoh,[a] Kohei Suruga,[a] Masahiro Ogawa,[a] Yasuhiro Isogai,[d] Toshiyuki Nishio,[a] Yoshitsugu Shiro[b] and Tadatake Oku[a]*

[a]Department of Biological Chemistry, College of Bioresource Sciences, Nihon University, 1866 Kameino, Fujisawa, Kanagawa 252-8510, Japan, [b]RIKEN Harima Institute/SPring-8, Mikazuki-cho, Sayo, Hyogo 679-5148, Japan, [c]Faculty of Science, Gakushuin University, Mejiro, Toshima-ku, Tokyo 170-0031, Japan, and [d]RIKEN, 2-1 Hirosawa, Wako, Saitama 351-0198, Japan

Correspondence e-mail: oku@brs.nihon-u.ac.jp

Received 10 August 2000
Accepted 18 October 2000

PDB Reference: cytochrome c_6, 1gdv.

The crystal structure of cytochrome c_6 from the red alga *Porphyra yezoensis* has been determined at 1.57 Å resolution. The crystal is tetragonal and belongs to space group $P4_32_12$, with unit-cell parameters $a = b = 49.26$ (3), $c = 83.45$ (4) Å and one molecule per asymmetric unit. The structure was solved by the molecular-replacement method and refined with *X-PLOR* to an R factor of 19.9% and a free R factor of 25.4%. The overall structure of cytochrome c_6 follows the topology of class I c-type cytochromes in which the heme prosthetic group covalently binds to Cys14 and Cys17, and the iron has an octahedral coordination with His18 and Met58 as the axial ligands. The sequence and the structure of the eukaryotic red algal cytochrome c_6 are very similar to those of a prokaryotic cyanobacterial cytochrome c_6 rather than those of eukaryotic green algal c_6 cytochromes.

1. Introduction

Cytochrome c_6 functions as an electron carrier between cytochrome b_6f complex and the P700 reaction center of photosystem I in some cyanobacteria and chloroplasts from eukaryotic algae. This protein is the functional counterpart of plastocyanin, a small copper protein, in chloroplasts from higher plants. Genes for both plastocyanin and cytochrome c_6 are present in some algal species and the alternative expression of the two proteins is regulated by the growth-condition copper availability (Sandmann *et al.*, 1983; Merchant & Bogorad, 1987). Although cytochrome c_6 and plastocyanin have approximately the same size (~10 kDa), similar redox potentials (~+370 mV) and isoelectric points (~4.5), these two proteins have no sequence similarity, contain different catalytic metals and are structurally unrelated to each other. Whereas plastocyanin is a β-sheet protein with copper as the central ion (Redinbo *et al.*, 1993), cytochrome c_6 is a highly α-helical heme-containing protein (Kerfeld *et al.*, 1995; Frazão *et al.*, 1995; Banci *et al.*, 1998; Beissinger *et al.*, 1998; Schnackenberg *et al.*, 1999).

Comparison of the amino-acid sequence allowed us to classify this cytochrome as a class I c-type cytochrome, in which the heme iron has methionine–histidine axial coordination (Kerfeld & Krogmann, 1998). Recently, crystal structures of cytochrome c_6 from the green algae *Chlamydomonas reinhardtii* (Kerfeld *et al.*, 1995), *Monoraphidium braunii* (Frazão *et al.*, 1995) and *Scenedesmus obliquus* (Schnackenberg *et al.*, 1999) have been determined. Solution structures of the protein from *M. braunii* (Banci *et al.*, 1998) and the thermophilic cyanobacterium *Synechococcus elongatus* (Beissinger *et al.*, 1998) have also been reported. These structural studies of c_6 cytochromes provide us with information about the structural relationship to other cytochromes

and plastocyanin, and about the mechanisms of the interactions with cytochrome *f* and photosystem I (Frazão *et al.*, 1995).

Although chloroplasts were thought to have evolutionally arisen from cyanobacteria (Aitken, 1976), there are differences in the expression and genome coding of cytochrome c_6 between green and red algae. In the green alga *C. reinhardtii*, the gene for cytochrome c_6 exists in the genomic DNA and its coding region is interrupted by two introns (Hill *et al.*, 1991). On the other hand, in the red alga *Porphyra purpurea*, the *pet*J gene encoding cytochrome c_6 exists in the chloroplast genome (Reith & Munholland, 1995). Physicochemical properties (visible absorptional maxima and redox potential) of cytochrome c_6 from the red alga *P. yezoensis* were reported by Sugimura *et al.* (1968) and are similar to those of other algal c_6 cytochromes. The cytochrome c_6 has 85 amino-acid residues and its sequence has been determined (Oku, PIR accession number JC5849). The amino-acid sequence of the *P. yezoensis* cytochrome c_6 shows a high similarity to that of the cyanobacterium rather than those of green algae (see §3). In order to investigate their structural relationships, we have determined the crystal structure of cytochrome c_6 from the red alga *P. yezoensis* and compared it with the structures of cyanobacterial and green algal c_6 cytochromes.

Table 1
Crystal parameters, data collection and structure refinement.

Values in parentheses are for the outer shell, with a resolution of 1.65–1.57 Å.

Data-collection statistics	
Temperature (K)	293
Resolution range (Å)	20.0–1.57
Space group	$P4_32_12$
Unit-cell parameters (Å)	$a = b = 49.26$ (3), $c = 83.45$ (4)
Reflections	
Measured	105068
Unique	14083
Completeness (%)	96.7 (95.0)
$R_{\rm merge}$† (%)	4.7 (34.7)
Redundancy	7.5 (7.5)
Mean $\langle I/\sigma(I)\rangle$	9.2 (2.2)
Refinement statistics	
Resolution range (Å)	20.0–1.57
Reflections used [$>0\sigma(F)$]	14061
R factor‡ (%)	19.9
Free *R* factor (%)	25.4
Total number of non-H atoms	677
Number of water molecules	45
R.m.s deviations from ideals	
Bond lengths (Å)	0.015
Bond angles (°)	1.586
Dihedral angles (°)	25.8
Improper angles (°)	1.43
Average *B* factors (Å^2)	
Main chain	27.9
Side chain	32.1
Heme molecules	15.4
Water molecules	42.0
Ramachandran plot	
Residues in most favorable regions (%)	83.8
Residues in additional allowed regions (%)	14.9
Residues in disallowed regions (%)	1.4

† $R_{\rm merge} = \sum|I_i - \langle I\rangle|/\sum I_i$, where I_i is the intensity of an observation and $\langle I\rangle$ is the mean value for its unique reflection; summations are over all reflections. ‡ *R* factor = $\sum_h|F_o(h) - F_c(h)|/\sum_h F_o(h)$, where F_o and F_c are the observed and calculated structure-factor amplitudes, respectively. The free *R* factor was calculated with 5% of the data excluded from the refinement.

2. Materials and methods

2.1. Purification and crystallization of the cytochrome c_6

Cytochrome c_6 was purified from frozen thalli of *P. yezoensis* obtained from Shirako Co. Ltd by ammonium sulfate fractionation and three steps of DEAE ion-exchange chromatography. The purified and lyophilized protein was dissolved in 5 m*M* sodium phosphate pH 7.0 to prepare a concentrated solution of 50 mg ml^{-1}. The cytochrome c_6 solution was mixed with an equal volume of 1.8 *M* ammonium sulfate buffered with 0.1 *M* sodium citrate pH 3.5. The cytochrome c_6 was crystallized at 293 K using the sitting-drop method; red bipyramidal crystals were obtained. The crystal parameters are given in Table 1.

2.2. Data collection and molecular replacement

X-ray diffraction data were obtained at the synchrotron-radiation source of the BL44B2 (RIKEN beamline 2) station at SPring-8, Harima, Japan (Adachi *et al.*, 1996). The data set was collected using an R-AXIS IV imaging plate as a detector. Measurements were performed at 293 K and a wavelength of 0.7 Å using a 0.2 mm collimator. Diffraction data were integrated and scaled with *MOSFLM* (Leslie, 1994) and *SCALA* (Collaborative Computational Project, Number 4, 1994). Statistics of the data collection are given in Table 1. The structure was solved by the molecular-replacement method. The rotation-funtion and translation searches were carried out using *X-PLOR* 3.851 (Brünger, 1993). The initial model for the *P. yezoensis* cytochrome c_6 structure was that of the cytochrome c_6 from *C. reinhardtii* (Kerfeld *et al.*, 1995; PDB code 1cyi) with the amino-acid sequence mutated to that of *P. yezoensis*. The rotation and translation functions were calculated using the native data (10.0–5.0 Å resolution), which yielded one molecule in an asymmetric unit with an *R* factor of 42.0%. The solution by molecular replacement was refined as a rigid body by the program *X-PLOR* 3.851 (Brünger, 1993); this was performed to further improve the orientation and positional parameters, which resulted in an *R* factor of 40.5% for 10.0–3.5 Å resolution data.

2.3. Refinement

The model was submitted to simulated-annealing (Brünger *et al.*, 1987) refinement using slow-cool protocols (Brünger *et al.*, 1990) from 3000 to 300 K with 10.0–2.0 Å resolution data. At this stage, the crystallographic *R* factor and the free *R* factor dropped to 31.6 and 35.2%, respectively. Subsequent cycles of rebuilding (manual model fitting using the program *TURBO-FRODO*; Roussel & Cambillau, 1989) followed by positional refinement and thermal parameter refinement with *X-PLOR* 3.851 (Brünger, 1993) were used to improve the model, as judged by free *R* factor. The high-resolution limit of the diffraction data was then increased from 2.0 to 1.57 Å in increments of 0.1 Å.

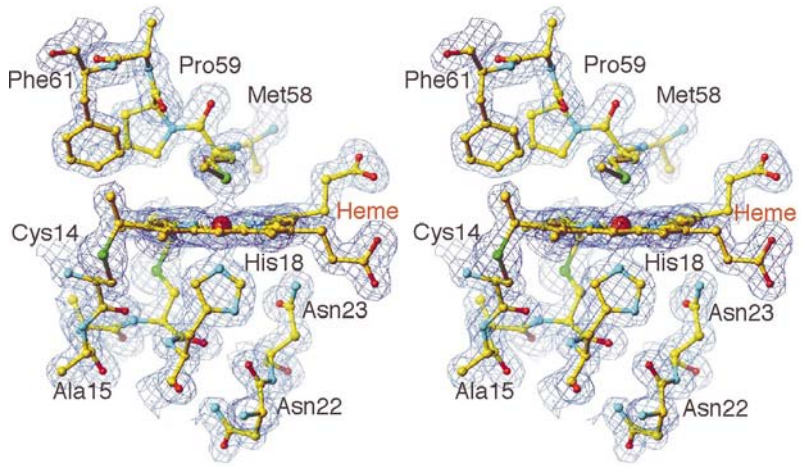

Figure 1
Stereoview of the final electron-density map ($2F_o - F_c$) around the heme of the cytochrome c_6 from *P. yezoensis*. The map was calculated with amplitudes of reflections in the resolution range 20.0–1.57 Å and is contoured at 1.3σ, where σ is the standard deviation of the electron-density map. The heme and neighboring residues are represented by ball-and-stick models with atom-specific colors: yellow, carbon; sky blue, nitrogen; red, oxygen; green, sulfur; dark red, iron.

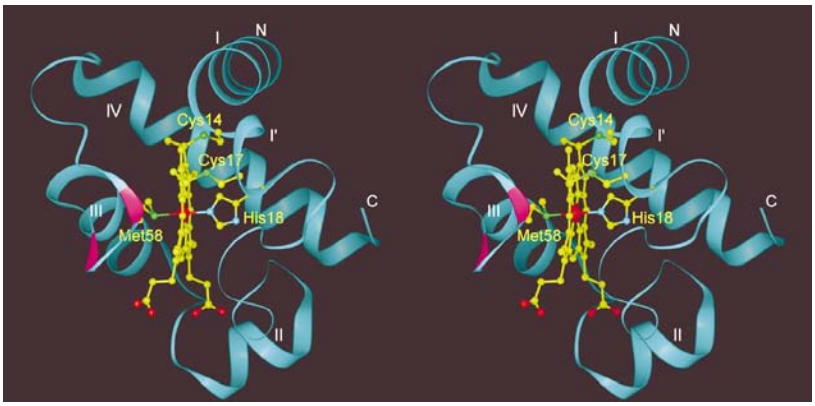

Figure 2
The overall structure of *P. yezoensis* cytochrome c_6. The helices and β-sheets (colored pink) are indicated as thick ribbons and the helices I–IV are numbered. The N- and C-termini are indicated. The heme prosthetic group and the heme-binding residues (Cys14, Cys17, His18 and Met58) are represented by ball-and-stick models in the same coloring scheme as Fig. 1. The figure is drawn with the solvent-exposed heme edge at the front (the His iron ligand being on the right).

At the final stage of *X-PLOR* 3.851 (Brünger, 1993) refinement, the low-resolution limit of the diffraction data was increased from 10.0 to 20.0 Å by applying a bulk-solvent correction (Jiang & Brünger, 1994). The water molecules were placed at positions where spherical densities were above 1.3σ in the $2F_o - F_c$ map and above 3.0σ in the $F_o - F_c$ map and where stereochemically reasonable hydrogen bonds were allowed. Structural evaluations of the final model of the cytochrome c_6 using *PROCHECK* (Laskowski *et al.*, 1993) indicated that 83.8% of the residues are in the most favourable regions of the Ramachandran plot. Fig. 1 shows the final electron-density map at 1.57 Å resolution superimposed upon the final model. The refined model included all residues (1–85) in each chain, heme and 45 water molecules, yielding an *R* factor of 19.9% and a free *R* factor of 25.4%. The r.m.s. deviations in bond lengths and angles were 0.015 Å and 1.586°, respectively. A summary of the refinement statistics is given in Table 1. Coordinates of the cytochrome c_6 have been deposited in the Protein Data Bank. For graphical presentations of the structure, *InsightII*98 (MSI) was used.

3. Results and discussion

3.1. Overall structure

The overall structure of *P. yezoensis* cytochrome c_6 follows the topology of class I *c*-type cytochromes (Fig. 2). *P. yezoensis* cytochrome c_6 consists of a single polypeptide chain folding around the heme prosthetic group. The spatial disposition of helices and β-sheets, as well as those of green algae and the cyanobacterium, resemble those of the bacterial *c* cytochromes *Pseudomonas aeruginosa* cytochrome *c*-551 (Matsuura *et al.*, 1982) and *Azotobacter vinelandii* cytochrome c_5 (Carter *et al.*, 1985) rather than mitochondrial *c* cytochromes, *e.g.* those of horse heart (Dickerson *et al.*, 1971), bonito (Tanaka *et al.*, 1975) and rice (Ochi *et al.*, 1983).

Secondary structures are classified according to the criteria of Kabsch & Sander (1983). Four α-helices, Asp2–Asn13 (I), Lys33–Ala38 (II), Ile44–Asn53 (III) and Asp67–Lys83 (IV), are observed as elements of regular secondary structure, with the arrangement of helices I and IV crossing with an angle of $\sim$90° (Fig. 2). Helices II and III are shorter than helices I and IV and reside on different sides relative to the heme plane, whereas those of mitochodrial *c* cytochromes are located on the side of the Met ligand. In addition to these α-helices, the region Ala15–His18, which is involved in the covalent bonds to the heme, forms a normal α-helix (I′) rather than the 3_{10}-helix observed in the corresponding region of the cyanobacterial cytochrome c_6 (Beissinger *et al.*, 1998).

Following the Ala15–His18 region, Gly20–Lys32 forms an Ω-shaped loop which is observed in other c_6 cytochromes (Kerfeld *et al.*, 1995; Frazão *et al.*, 1995; Beissinger *et al.*, 1998) and contributes to the structural stabilization of this region (Leszczynski & Rose, 1986). This is achieved by three main-chain and one side-chain hydrogen bonds; the amide groups of Lys29 and Leu31 and $N^{\delta 2}$ of Asn23 form hydrogen bonds with the carbonyl O atoms of Met26, Gly21 and Lys29, respectively (Table 2).

The sixth ligand, the Met58 residue, is a part of the region stretching from Gly54 to Val66 which separates the helix III from the helix IV. A short β-sheet in the vicinity of Met58 is located in this segment (Fig. 2). This two-stranded antiparallel

Table 2
Hydrogen bonds not involved in the helices I–IV.

MC, main-chain; SC, side-chain.

Region	MC···MC	Distance (Å)	MC···SC	Distance (Å)
14–32	Phe10 O···Ala15 N	2.97	Asn22 O···His18 $N^{\delta1}$	2.79
	Cys17 O···Ala24 N	2.90	Lys29 O···Asn23 $N^{\delta2}$	2.91
	His18 O···Gly21 N	2.68	Leu31 O···Trp85 $N^{\varepsilon1}$	2.94
	Gly21 O···Leu31 N	2.76		
	Met26 O···Lys29 N	2.92		
54–66	Val51 O···Phe61 N	2.82		
	Gln52 O···Gly62 N	3.04		
	Lys55 O···Met58 N	2.90		
	Met58 O···Lys55 N	3.00		
	Phe61 O···Leu65 N	2.73		
	Val66 O···Asp69 N	2.83		
83–85	Gln80 O···Trp85 N	2.97		

β-sheet (residues 55–58) is formed by only two main-chain hydrogen bonds between Lys55 and Met58 (Lys55 N and Met58 O, Lys55 O and Met58 N) which form a type II′ β-turn with residues Asn56 and Ala57 (Table 2). This short β-sheet has been observed in the structures of other c_6 cytochromes (Kerfeld *et al.*, 1995; Frazão *et al.*, 1995; Banci *et al.*, 1998; Beissinger *et al.*, 1998; Schnackenberg *et al.*, 1999) as well as that of cytochrome c_5 from *A. vinelandii* (Carter *et al.*, 1985). In the structures of mitochondrial cytochrome *c*, this region has no β-sheet (Tanaka *et al.*, 1975; Ochi *et al.*, 1983; Bushnell *et al.*, 1990).

On the His18 side of the heme group, the conserved residues Phe10, Tyr76 and Trp85 form a triangular aromatic stack neighboring pyrrole ring B of the heme. The triangular aromatic stack is observed in other c_6 cytochromes (Kerfeld *et al.*, 1995; Frazão *et al.*, 1995; Beissinger *et al.*, 1998). The phenylalanine at position 10 within helix I, which is highly conserved in all class I *c*-type cytochromes, interacts with another aromatic residue at the position 76 and stabilizes the interaction between helices I and IV. The association of these helices has been proposed to be an early event in the folding pathway for class I *c*-type cytochromes (Bushnell *et al.*, 1990).

3.2. Heme environment structure

The heme prosthetic group covalently binds to the polypeptide chain with two thioether bonds from Cys14 and Cys17 and is almost entirely buried within a hydrophobic crevice (Figs. 1 and 2). The structure of the heme is slightly distorted into a saddle shape, which is typical of *c*-type cytochrome heme prosthetic groups.

The iron of the heme has an octahedral coordination with His18 and Met58 as the axial ligands (Fig. 2); the distances of the axial coordinated atoms His18 $N^{\varepsilon2}$ and Met58 S^{δ} from the heme iron are 2.07 Å and 2.35 Å, respectively, and the angle His18 $N^{\varepsilon2}$—Fe—Met58 S^{δ} is 177.65°. His18 $N^{\delta1}$ forms a hydrogen bond with the carbonyl O atom of the Asn22 main chain (Table 2). In other class I *c* cytochromes, $N^{\delta1}$ of the ligand His forms a hydrogen bond to the carbonyl O atom of a conserved proline (Tanaka *et al.*, 1975; Matsuura *et al.*, 1982; Ochi *et al.*, 1983; Carter *et al.*, 1985; Bushnell *et al.*, 1990). The S atom (S^{δ}) of the axial ligand methionine forms no hydrogen bond in the cytochrome c_6, as in the other algal c_6 cytochromes and *A. vinelandii* cytochrome c_5 (Carter *et al.*, 1985). This is in contrast to mitochondrial cytochrome *c* structures, in which the Met S^{δ} forms a hydrogen bond to Tyr67 OH (Bushnell *et al.*, 1990).

Although the mitochondrial *c* cytochromes have some conserved water molecules in the heme crevice (Berghuis, Guillemette, McLendon *et al.*, 1994; Berghuis, Guillemette, Smith *et al.*, 1994), no such water molecules are found in the heme crevice of the *P. yezoensis* cytochrome c_6. Instead, it has only two water molecules, Wat17 and Wat33, located between the propionates of pyrrole rings A and D (Fig. 3). Wat17 has also been observed at the corresponding position in other cytochromes c_6. Wat17 forms hydrogen bonds with Gln50 $O^{\varepsilon1}$, propionate O1D of the heme pyrrole ring D and Wat33, which also forms a hydrogen bond with the propionate O1A of the heme pyrrole ring A. The conserved water molecule Wat17 seems to play no significant role in the redox cycle, since it exists in this position in both the reduced and oxidized forms (Schnackenberg *et al.*, 1999). However, both water molecules may contribute to the stabilization of the structure around the heme as well as the fixation of the conformations of the propionate group of pyrrole ring D and the side chain of Gln50.

Unlike the horse heart cytochrome *c*, which shows a positively charged front surface (Bushnell *et al.*, 1990), *P. yezoensis* cytochrome c_6, in common with other algal c_6 cytochromes, exhibits no such positively charged region. The surface surrounding the solvent-exposed heme pyrrole ring C and the propionate of the heme pyrrole ring D is characterized by uncharged residues: Asn13, Ala16, Ile25, Met26, Asn57, Pro59 and Phe61. These residues create a hydrophobic patch which embraces the heme prosthetic group. Asn13, Ala16, Ile25 and Asn56 of these residues structurally correspond to Lys13, Gln16, Thr28 and Lys79 of horse cytochrome *c*, respectively.

Cytochrome c_6 has a higher redox potential (approximately +370 mV) than its mitochondrial counterpart (+260 mV). Kerfeld *et al.* (1995) proposed that the difference in redox potential between cytochromes c_6 and *c* can be attributed to the difference in hydrogen-bond formation of the ligand atoms, as mentioned above, and the ionization of the solvent-exposed propionate of the heme pyrrol ring D. We suggest an additional reason for the difference in the redox properties. Water molecules near the heme iron generally stabilize its ferric form and thus lower the redox potential (Kassner, 1973). As mentioned above, the heme environment of cytochrome c_6 is less polar than that of the mitochondrial counterpart and thus no water molecule is present in the heme crevice, in contrast to mitochondrial cytochrome *c* which has some conserved water molecules. Therefore, the heme hydrophobic patch of the cytochrome c_6 should contribute to the enhancement of redox potential.

The edge of pyrrole ring C and the propionate side chain of pyrrole ring D are exposed to the solvent (Figs. 2 and 3) and are thought to form the path of direct electron transfer from the heme to potential electron-transfer partners (Frazão *et al.*,

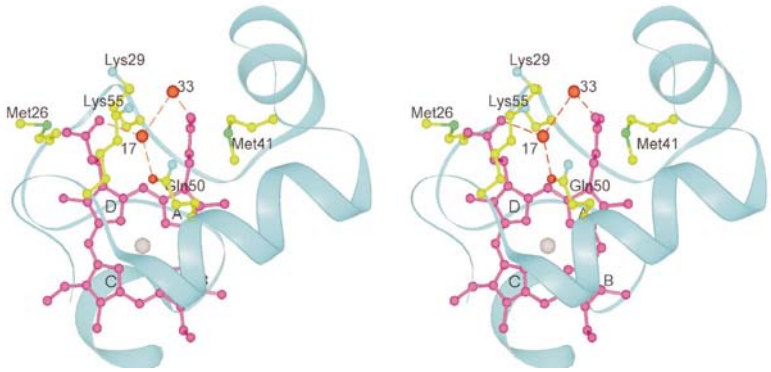

Figure 3
The structure around the exposed heme edge of the cytochrome c_6. The ribbon model shows the protein region (residues 14–59). The heme is represented in pink and the heme iron by a grey ball. Met26, Lys29, Met41, Gln50 and Lys55 are represented by ball-and-stick models in the same coloring scheme as Fig. 1. Water molecules are represented as red balls. Possible hydrogen bonds are indicated by red dashed lines.

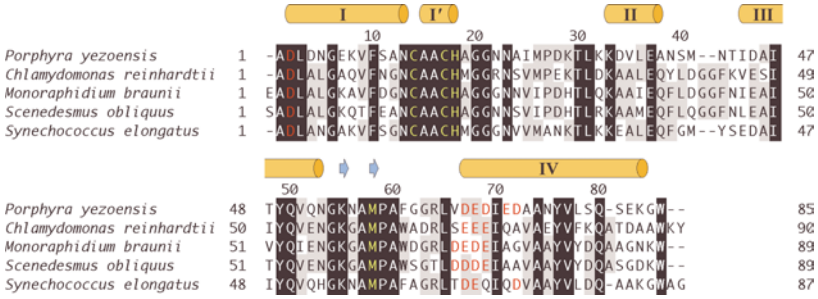

Figure 4
Sequence alignment of c_6 cytochromes whose crystal structures have been reported. The conserved and semi-conserved amino-acid residues among five algal species are indicated with black and grey boxes, respectively. The heme ligands and the residues forming the acidic patch of the exposed surface of the C-terminal helix are colored yellow and red, respectively. The secondary structures of cytochrome c_6 of *P. yezoensis* are indicated: orange cylinders, helices; blue arrows, β-sheets. The PIR accession numbers of the cited sequences are as follows: *P. yezoensis*, JC5849; *C. reinhartii*, CCKM6R; *M. braunii*, S35677; *S. obliquus*, S77923; *S. elongatus*, P56534.

Figure 5
Comparison of *P. yezoensis* (pink), *S. obliquus* (green; PDB code 1c6o) and *S. elongatus* (blue; PDB code 1c6s) c_6 cytochromes in tube representation. The view is drawn in the same direction as that in Fig. 2. The loop regions around residue 40, the region following helix II, of *P. yezoensis* and *S. elongatus* c_6 cytochromes are different from that of the *S. obliquus* protein.

1995; Ullmann *et al.*, 1997). Although the area around the heme is non-polar, two basic residues, Lys29 and Lys55, flank the long axis of the exposed heme crevice about pyrrole ring D (Fig. 3). Mitochondrial cytochrome *c* also has two basic residues flanking the exposed portion of the heme. Thus, these residues may be critical for the function since they are conserved in both cytochromes c_6 and *c*, despite the large difference in the isoelectric point: cytochrome c_6 has a pI of 4, whereas mitochondrial cytochrome *c* has a pI of ∼10. In mitochondrial cytochrome *c*, at least one of these Lys residues is important for interaction with both physiological redox partners. Moreover, modification of these positively charged residues with small-molecule reagents affects the rate of electron transfer (Ahmed & Millett, 1981; Butler *et al.*, 1983).

3.3. Comparison with other algal cytochrome c_6 structures

Presently, the three-dimensional structures of c_6 cytochromes from the green algae *C. reinhardtii* (Kerfeld *et al.*, 1995), *M. braunii* (Frazão *et al.*, 1995; Banci *et al.*, 1998) and *Scenedesmus obliquus* (Schnackenberg *et al.*, 1999) as well as the cyanobacterium *Synechococcus elongatus* (Beissinger *et al.*, 1998) are known. Like cytochrome c_6 from *P. yezoensis*, they comprise 85–90 amino-acid residues and their main secondary-structural elements are α-helices wrapping around the heme prosthetic group. Sequence comparisons between c_6 cytochromes from *P. yezoensis* and *C. reinhardtii*, *M. braunii*, *S. obliquus* and *S. elongatus* revealed similarities of 46.67, 51.11, 51.69 and 65.52%, respectively (Fig. 4).

Despite the high overall similarity of the structures (Fig. 5), subtle differences exist. The largest deviation is observed in the loop region around residue 40, where the green algal proteins have a small insertion of two amino acids compared with the *P. yezoensis* cytochrome c_6. The loop region in the *P. yezoensis* cytochrome c_6 resembles that in the cyanobacterial cytochrome c_6, which also lacks two amino acids in this region compared with green algal c_6 cytochromes (Figs. 4 and 5). The similarity of the sequence in the region of residues 40–45 is relatively low compared with the similarity in the other regions of the cytochrome c_6 sequence. Therefore, this region may have no common functional role. In three-dimensional structures of other c_6 cytochromes, functional roles for this region have not been found.

Met26 and Met41 are conserved between *P. yezoensis* and *S. elongatus* and the heme crevice is flanked by their side chains (Figs. 3 and 4). These residues were suggested to act as endogenous antioxidants when they are arranged to guard the active site from oxidants (Levine *et al.*, 1996). The suggestion is in good agreement with our observation that the *P. yezoensis* cytochrome c_6 possesses resistance to auto-oxidation.

At the surface exposed to the solvent around the C-terminal helix IV, a negatively charged region consisting of Asp2, Asp67, Glu68, Asp69, Glu71, and Asp72 is observed (Fig. 4). In other algal c_6 cytochromes, a similar charge distribution is also found. This region seems to play a functional role in the interaction between cytochrome c_6 and its redox partners (Frazão *et al.*, 1995; Kerfeld *et al.*, 1995; Ullmann *et al.*, 1997). One of them is cytochrome *f*, which has positively charged zones located in the small domain containing lysines and arginines (Martinez *et al.*, 1994) and the other is the PsaF subunit of photosystem I which has a positively charged N-terminal α-helix containing six lysines (Hippler *et al.*, 1996). Cytochrome c_6 and plastocyanin should interact with these regions of cytochrome *f* and photosystem I.

Red alga has been proposed to be the earliest eukaryotic organism and to be an ancestor of the higher plants (Stiller & Hall, 1997). It is only in red algae that the cytochrome c_6 gene is encoded in the chloroplast genome (Reith & Munholland, 1995), while the green algal counterpart is encoded in the nuclear gene (Hill *et al.*, 1991). High similarities in amino-acid sequence and three-dimensional structure of cytochrome c_6 between red algae and cyanobacteria were observed in this study as well as in previous reports (Ambler & Bartsch, 1975; Aitken, 1976). Thus, the present results support the hypothesis that the red alga is the missing link between the higher plants and the most ancient photosythetic eukaryotic organisms.

TO thanks Dr Makoto Yaguchi of the National Research Council of Canada (Ottawa) for valuable discussions. This work was supported in part by Grants-in-Aid for Research for the Future Program (JSPS-RFTF97R16001) from the Japan Society for the Promotion of Science and for Exploratory Research from the Ministry of Education, Science, Sports and Culture of Japan.

References

Adachi, S., Oguchi, T. & Ueki, T. (1996). SPring-8 Annual Report, pp. 239–240.
Ahmed, A. J. & Millett, F. (1981). *J. Biol. Chem.* **256**, 1611–1615.
Aitken, A. (1976). *Nature (London)*, **263**, 793–796.
Ambler, R. P. & Bartsch, R. G. (1975). *Nature (London)*, **253**, 285–288.
Banci, L., Bertini, I., De la Rosa, M. A., Koulougliotis, D., Navarro. J. A. & Walter, O. (1998). *Biochemistry*, **37**, 4831–4843.
Beissinger, M., Sticht, H., Sutter, M., Ejchart, A., Haehnel, W. & Rösch, P. (1998). *EMBO J.* **17**, 27–36.
Berghuis, A. M., Guillemette, J. G., McLendon, G., Shermen, F., Smith, M. & Brayer, G. D. (1994). *J. Mol. Biol.* **236**, 786–799.
Berghuis, A. M., Guillemette, J. G., Smith, M. & Brayer, G. D. (1994). *J. Mol. Biol.* **235**, 1326–1341.
Brünger, A. T. (1993). *X-PLOR: Version 3.1. A System for Crystallography and NMR.* New Haven, CT, USA: Yale University Press.
Brünger, A. T., Krukowski, A. & Erickson, J. (1990). *Acta Cryst.* A**46**, 585–593.
Brünger, A. T., Kuriyan, J. & Karplus, M. (1987). *Science*, **235**, 458–460.
Bushnell, G. W., Louie, G. V. & Brayer, G. D. (1990). *J. Mol. Biol.* **214**, 585–595.
Butler, J., Chapman, S. K., Davies, D. M., Sykes, A. G., Speck, S. H., Osheroff, N. & Margoliash, E. (1983). *J. Biol. Chem.* **258**, 6400–6404.
Carter, D. C., Melis, K. A., O'Donnell, S. E., Burgess, B. K., Furey, W. F. Jr, Wang, B.-C. & Stout, C. D. (1985). *J. Mol. Biol.* **184**, 279–295.
Collaborative Computational Project, Number 4 (1994). *Acta Cryst.* D**50**, 760–763.
Dickerson, R. E., Takano, T., Eisenberg, D., Kallai, O. B., Samson, L., Cooper, A. & Margoliash, E. (1971). *J. Biol. Chem.* **246**, 1511–1535.
Frazão, C., Soares, C. M., Carrondo, M. A., Pohl, E., Dauter, Z., Wilson, K. S., Hervás, M., Navarro, J. A., De la Rosa, M. A. & Sheldrick, G. M. (1995). *Structure*, **3**, 1159–1169.
Hill, K. L., Li, H. H., Singer, J. & Merchant, S. (1991). *J. Biol. Chem.* **266**, 15060–15067.
Hippler, M., Reichert, J., Sutter, M., Zak, E., Altschmied, L., Schröer, U., Hermann, R. G. & Haehnel, W. (1996). *EMBO J.* **15**, 6374–6384.
Jiang, J.-S. & Brünger, A. T. (1994). *J. Mol. Biol.* **243**, 100–115.
Kabsch, W. & Sander, C. (1983). *Biopolymers*, **22**, 2577–2637.
Kassner, R. J. (1973). *J. Am. Chem. Soc.* **95**, 2674–2677.
Kerfeld, C. A., Anwar, H. P., Interrante, R., Merchant, S. & Yeates, T. O. (1995). *J. Mol. Biol.* **250**, 627–647.
Kerfeld, C. A. & Krogmann, D. W. (1998). *Annu. Rev. Plant Physiol. Plant Mol. Biol.* **49**, 397–425.
Laskowski, R. A., MacArthur, M. W., Moss, D. S. & Thornton, J. M. (1993). *J. Appl. Cryst.* **26**, 283–291.
Leslie, A. G. W. (1994). *MOSFLM Users Guide.* MRC-LMB, Cambridge, UK.
Leszczynski, J. F. & Rose, G. D. (1986). *Science*, **234**, 849–855.
Levine, R. L., Mosoni, L., Berlett, B. S. & Stadtman, E. R. (1996). *Proc. Natl. Acad. Sci. USA*, **93**, 15036–15040.
Martinez, S. E., Huang, D., Szczepaniak, A., Cramer, W. A. & Smith, J. L. (1994). *Structure*, **2**, 95–105.
Matsuura, Y., Takano, T. & Dickerson, R. E. (1982). *J. Mol. Biol.* **156**, 389–409.
Merchant, S. & Bogorad, L. (1987). *J. Biol. Chem.* **262**, 9062–9067.
Ochi, H., Hata, Y., Tanaka, N., Kakudo, M., Sakurai, T., Aihara, S. & Morita, Y. (1983). *J. Mol. Biol.* **166**, 407–418.
Redinbo, M. R., Cascio, D., Choukair, M. K., Rice, D., Merchant, S. & Yeates, T. O. (1993). *Biochemistry*, **32**, 10560–10567.
Reith, M. & Munholland, J. (1995). *Plant Mol. Biol. Rep.* **13**, 333–335.
Roussel, A. & Cambillau, C. (1989). *Silicon Graphics Geometry Partner Directory*, edited by Silicon Graphics, pp. 77–78. Mountain View, California: Silicon Graphics.
Sandmann, G., Reck, H., Kessler, E. & Böger, P. (1983). *Arch. Microbiol.* **134**, 23–27.
Schnackenberg, J., Than, M. E., Mann, K., Wiegand, G., Huber, R. & Reuter, W. (1999). *J. Mol. Biol.* **290**, 1019–1030.
Stiller, J. W. & Hall, B. D. (1997). *Proc. Natl Acad. Sci. USA*, **94**, 4520–4525.
Sugimura, Y., Toda, F., Murata, T. & Yakushiji, E. (1968). *Structure and Function of Cytochromes*, edited by K. Okunuki, M. D. Kamen & I. Sekuzu, pp. 452–458. Tokyo University Press.
Tanaka, N., Yamane, T., Tsukihara, T., Ashida, T. & Kakudo, M. (1975). *J. Biochem. (Tokyo)*, **77**, 147–162.
Ullmann, G. M., Hauswald, M., Jensen, A., Kostíc, N. M. & Knapp, E. W. (1997). *Biochemistry*, **36**, 16187–16196.